Secretory Proteins as Potential Semiochemical Carriers in the Horse†

Barbara D'Innocenzo,‡ Anna Maria Salzano,§ Chiara D'Ambrosio,§ Angelo Gazzano,|| Alberto Niccolini,|| Carlo Sorce,⊥ Francesca Romana Dani,@ Andrea Scaloni,§ and Paolo Pelosi*,‡

Dipartimento di Chimica e Biotecnologie Agrarie, Università di Pisa, 56124 Pisa, Italy, Laboratorio di Proteomica e Spettrometria di Massa, ISPAAM, Consiglio Nazionale delle Ricerche, 80147 Napoli, Italy, Dipartimento di Anatomia, Biochimica e Fisiologia Veterinaria, Università di Pisa, Pisa, Italy, Dipartimento di Biologia delle Piante Agrarie, Università di Pisa, Pisa, Italy, and Centro Interdipartimentale di Spettrometria di Massa, Università di Firenze, Firenze, Italy

Received July 13, 2006; Revised Manuscript Received August 19, 2006

ABSTRACT: Two soluble proteins were isolated as major secretory products of horse sweat and of the parotid gland and characterized for structural and functional properties. The first protein, lipocalin allergen EquC1, was characterized for its glycosylation sites and bound glycosidic moieties. Only one (Asn53) of the two putative glycosylation sites within the sequence was post-translationally modified; a different glycosylation pattern was determined with respect to data previously reported. When purified from horse sweat, this protein contained oleamide and other organic molecules as natural ligands. Ligand binding experiments indicated good protein selectivity toward volatile compounds having a straight chain structure of 9−11 carbon atoms, suggesting a role of this lipocalin in chemical communication. The second protein, here reported for the first time in the horse, belongs to the group of parotid secretory proteins, part of a large superfamily of binding proteins whose function in most cases is still unclear. This protein was sequenced and characterized for its post-translational modifications. Of the three cysteine residues present, two were involved in a disulfide bridge (Cys155−Cys198). A model, built up on the basis of similar proteins, indicated a general fold characterized by the presence of a long hydrophobic barrel. Binding experiments performed with a number of different organic compounds failed to identify ligands for this protein with a well-defined physiological role.

Chemical communication in vertebrates often utilizes soluble proteins as pheromone carriers (*1*, *2*). These proteins are secreted into main biological fluids, such as urine and saliva, and carry chemicals as endogenous ligands, having proven or potential activity as specific pheromones. A few examples have been studied in detail, including mouse and rat urinary proteins (*3*−*7*), hamster vaginal secretory proteins (*8*−*10*), pig salivary proteins (*11*−*14*), and human sweat proteins (*15*).

Major urinary (MUPs)[1] and α2u proteins are lipocalins that were first described in mouse and rat, which are synthesized in the liver and excreted in the urine (*16*, *17*). Subsequently, expression of members of this protein family was reported in salivary, lachrymal, and mammary glands (*18*). The physiological role of these polypeptides remained unknown until the discovery of odorant-binding proteins (OBPs) in the nasal tissue of several vertebrates provided evidence of a strong similarity between members of the two families (*19*, *20*). In some cases, the same genes have been found to be expressed both in the nose and in the liver (*21*). Apart from the site of expression, what differentiates OBPs and MUPs are endogenous ligands, present only in the latter, that have been recognized as species-specific pheromones. The role of MUPs in chemical communication between sexes is further confirmed by the selective expression of these proteins, whose synthesis is under hormonal control, only in adult males, being absent in females as well as in young or castrated individuals.

Proteins of the same family are abundantly secreted from the submaxillary glands of the adult mature boar, being completely absent in the sow and in castrated pigs. Again, such salivary lipocalins (SALs) contain two components of the boar sex pheromonal system as endogenous ligands, namely, 5α-androst-16-en-3-one and 5α-androst-16-en-3α-ol (*11*). The same proteins are also expressed in the nasal tissue of both sexes in the pig, but in that case, they are devoid of ligands (*13*). Aphrodisin is another lipocalin secreted in the vaginal fluid of the hamster (*8*−*10*, *22*). Also in this case, a bound volatile molecule, 1-hexadecanol, has been purified from the same fluid and suggested to be the protein's endogenous ligand (*23*). Finally, a potent odorant

† This work was partially supported by grants from MIUR (FIRB 2001, RBAU01PRLA, and RBAU01T97W) and CNR (Agroalimentare, Commessa 404).

* To whom correspondence should be addressed: Dipartimento di Chimica e Biotecnologie Agrarie, University of Pisa, Via S. Michele, 4, 56124 Pisa, Italy. Telephone: +39 050 2216626. Fax: +39 050 2216630. E-mail: ppelosi@agr.unipi.it.

‡ Dipartimento di Chimica e Biotecnologie Agrarie, Università di Pisa.

§ Consiglio Nazionale delle Ricerche.

|| Dipartimento di Anatomia, Biochimica e Fisiologia Veterinaria, Università di Pisa.

⊥ Dipartimento di Biologia delle Piante Agrarie, Università di Pisa.

@ Università di Firenze.

[1] Abbreviations: ESI, electrospray ionization; LPS, lipopolysaccharide binding protein; LTP, lipid transfer protein; MALDI-TOF, matrix-assisted laser desorption ionization time-of-flight; MUP, major urinary protein; MS, mass spectrometry; 1-NPN, *N*-phenyl-1-naphthylamine; OBP, odorant-binding protein; PLUNC, palate, lung, and nasal epithelial clone; PSP, parotid secretory protein; SAL, salivary lipocalin.

10.1021/bi061409p CCC: $33.50
Published on Web 10/24/2006

of human sweat, 3-methyl-2-heptenoic acid, is carried by another lipocalin called apoliprotein-D, abundantly produced in the sweat under certain conditions (*10*, *24*).

On the basis of the evidence accumulated so far in different species, indicating that sweat and saliva can be involved in chemical communication with conspecifics, we decided to investigate the presence of protein carriers for pheromones in such secretions. The most abundant protein of horse sweat, EquC1, is a lipocalin and has been reported to be an allergen (*25*−*28*). Here we report the characterization of EquC1 in terms of structural properties and ligand binding activity with respect to a series of organic compounds that are potential semiochemicals. Our data suggest that such a lipocalin could be a pheromone carrier in the horse, analogous with urinary and salivary lipocalins from other species. In all three major salivary glands, we also identified a protein with a sequence similar to that of parotid salivary proteins (PSPs) (*29*−*34*), a subset of a larger family, including LPS/LTP/PLUNC (*35*) and BPI genes (*36*), with members expressed in the nasal, oral, airway, and digestive epithelia, as well as in lachrymal glands (*37*). Some similarity was also observed with proteins of the nasal tissue of the rat (*38*) and vomeromodulin (*39*), whose functions are still unclear. Molecular modeling studies were suggestive of a structural fold compatible with a protein ligand binding function for long linear organic molecules.

MATERIALS AND METHODS

Reagents. Sequencing-grade proteases were purchased from Roche. Ultrapure HPLC-grade solvents were from Baker. Taq polymerase was from Amersham. Oligonucleotides were custom synthesized at Invitrogen. All other chemicals, including the ligands used in binding assays, were purchased from Sigma-Aldrich and were reagent-grade.

Preparation of Extracts. Samples of three major salivary glands were obtained from a local abattoir; sweat was collected from all over the body of male and female horses. All samples were kept at −20 °C for 1−2 days before extraction of proteins. Tissue samples were homogenized in ∼5 volumes of 50 mM Tris-HCl (pH 7.4) using a blender. Sweat samples were diluted in 5 volumes of the same buffer. Extracts were prepared by centrifugation of the homogenates at 10 000 rpm for 30 min, at 4 °C, and used for protein purification and Western blot analysis.

Protein Purification. PSP was purified from male horse parotid by precipitation from a crude extract with 45% (w/v) ammonium sulfate, followed by anion-exchange chromatography on a DE-52 or Mono-Q resin. Similarly, EquC1 was directly purified from concentrated horse sweat using the same chromatographic system. In all cases, columns were equilibrated in 50 mM Tris-HCl (pH 7.4), and samples were eluted in the same buffer with a linear gradient of 0 to 0.5 M NaCl. Fractions were assayed by SDS−PAGE.

Preparation of Antisera. Antisera were obtained by injecting an adult rabbit subcutaneously and intramuscularly with 500 μg of native protein, followed by two additional injections of 300 μg after 15 and 30 days. The protein was emulsified with an equal volume of Freund's complete adjuvant for the first injection and incomplete adjuvant for further injections. Animals were bled 10 days after the last injection, and the serum was used without further purification. Rabbits were individually housed in large cages, at constant temperature, and all operations were performed according to ethical guidelines to minimize pain and discomfort to the animals.

Western Blot Analysis. After electrophoretic separation under denaturing conditions, proteins were electroblotted on a nitrocellulose membrane, using the procedure of Kyhse-Andersen (*40*). After being treated with 0.2% (w/v) dried milk and 0.05% (w/v) Tween 20 in PBS, overnight, the membrane was incubated with the crude antiserum against the protein (1:500 dilution) and then with a goat anti-rabbit IgG−horseradish peroxidase conjugate (1:1000 dilution). Immunoreactive bands were detected by treatment with 4-chloro-1-naphthol.

Protein Alkylation. Protein samples were alkylated with 1.1 M iodoacetamide in 0.25 M Tris-HCl, 1.25 mM EDTA, and 6 M guanidinium chloride (pH 7.0) containing a 20-fold molar excess of dithiothreitol, at room temperature, for 1 min, in the dark. Parallel experiments were performed in the same buffer, but in the absence of a reducing agent. Proteins were freed from salt and reagent excess by passing the reaction mixture through a narrow bore Vydac C_4 column, as previously reported (*41*). Protein samples were manually collected and lyophilized.

Enzymatic Hydrolysis. Protein samples were digested with trypsin or endoproteinase AspN in 50 mM ammonium bicarbonate at pH 8.0 and 37 °C, overnight, using an enzyme: substrate ratio of 1:100 (w/w). Digests were directly analyzed by MALDI-TOF-MS following μZipTipC_{18} desalting and/or separated on a Vydac C_{18} 218TP52 column (250 mm × 1 mm, 5 μm, 300 Å pore size) (The Separation Group, Hesperia, CA), using a linear gradient from 5 to 60% acetonitrile containing 0.1% TFA, over a period of 70 min, at a flow rate of 0.05 mL/min. Peptide fractions were manually collected and lyophilized.

Protein Sequence Analysis. Automated N-terminal degradation of protein or peptide samples was performed by using a Procise 491 protein sequencer (Applied Biosystems) equipped with a 140C microgradient apparatus and a 785A UV detector (Applied Biosystems) for the automated identification of PTH-bound amino acids.

Protein Mass Spectrometry Analysis. ESI mass spectra of intact proteins were recorded by using an API-100 single-quadrupole mass spectrometer (Applied Biosystems) equipped with an atmospheric pressure ionization source as previously reported (*41*). Mass calibration was performed by means of the multiply charged ions from a separate injection of horse heart myoglobin (molecular mass of 16 951.5 Da). All masses are reported as average values.

MALDI-TOF mass spectra of whole protein digests or individual peptide fractions were recorded using a Voyager DE-PRO mass spectrometer (Applied Biosystems) as previously reported (*42*). A mixture of the analyte, α-cyano-4-hydroxycinnamic acid, and internal standards was loaded on the instrument target, using the dried droplet technique. Spectra were recorded in either reflectron or linear mode. Assignment of recorded mass values to individual peptides was performed on the basis of their molecular mass, protein sequence, and protease specificity.

RNA Extraction and cDNA Synthesis. Total RNA was extracted from the parotid gland of an adult female horse using the TRI Reagent (Sigma), following the manufacturer's protocol. cDNA was prepared from total RNA by reverse

transcription, using 200 units of SuperScript III Reverse Transcriptase (Invitrogen) and 0.5 μg of a primer containing an oligo-dT preceded by a specific sequence (5′-ATTCTA-GAGCGGCCGCGACATGT$_{14}$-3′) in a total volume of 50 μL. The mixture also contained dNTPs (0.5 mM each) (Pharmacia Biotech, Uppsala, Sweden), 75 mM KCl, 3 mM $MgCl_2$, 10 mM DTT, and 0.1 mg/mL BSA in 50 mM Tris-HCl (pH 8.3). The reaction mixture was incubated at 50 °C for 60 min, and the product was directly used for PCR amplification or stored at −20 °C.

Polymerase Chain Reaction. Aliquots of 1 μL of crude cDNA were amplified in a Bio-Rad Gene CyclerTM thermocycler, using 2.5 units of *Thermus aquaticus* DNA polymerase (Pharmacia Biotech), dNTPs (1 mM each) (Pharmacia Biotech), PCR primers (1 μM each), 50 mM KCl, 2.5 mM $MgCl_2$, and 0.1 mg/mL BSA in 10 mM Tris-HCl (pH 8.3) containing 0.1% (v/v) Triton X-100. At the 5′ end, we used a forward degenerate primer designed on the first 11 amino acids of PSPs from other species (5′-ATGBT-TCARCTTTGGAAACTTGTTYTCYTGTG-3′). At the 3′ end, we used the same primer adopted for the synthesis of cDNA. After a denaturing step at 95 °C for 5 min, the reaction was performed for 35 cycles (95 °C for 1 min, 44 °C for 1 min, and 68 °C for 1 min), followed by a final step at 72 °C for 7 min. We thus obtained an amplification product of ~1100 bp.

Cloning and Sequencing. The crude PCR products were ligated into a pGEM vector without further purification, using a 1:5 (plasmid:insert) molar ratio and by incubating the mixture overnight at room temperature. After transformation of *Escherichia coli* XL-1 Blue competent cells with the ligation product, positive colonies were selected by PCR using the plasmid's primers SP6 and T7 and grown in LB/ampicillin medium. DNA was extracted and custom sequenced at MWG (Martinsried, Germany).

Sequence Analysis and Molecular Modeling. A computer-assisted scan for the occurrence of specific sequence patterns, profiles, and post-translational modification motifs was obtained with ScanProsite (*43*). Protein fold recognition analysis was performed with 3D-PSSM (*44*), which identified human bactericidal permeability-increasing protein (*45*) as the unique protein present in Protein Data Bank presenting a similar structural and domain organization. Pairwise sequence alignment was initially conducted with SIM (*46*), further subjected to manual adjustments on the basis of the predicted (horse parotid protein) (*47*, *48*) and observed (human PBI) (*49*) protein secondary structure. Computer modeling was performed on a Silicon Graphics O2 workstation. The three-dimensional model of horse parotid protein was constructed on the basis of the 1.7 Å crystallographic structure of human bactericidal permeability-increasing protein (PDB entry 1EWF) using the sequence alignment obtained as described above. The horse parotid protein N-terminal fragment (residues 1−41) and the C-terminal dodecapeptide were not included in model construction because of their poor sequence homology with human PBI. The three-dimensional model was constructed with the Insight/Homology program package (Biosym). Several cycles of constrained energy minimization regularized the structure and geometrical parameters. The model was validated using WHATCHECK (*50*).

GC−MS Analysis of Endogenous Ligands. Aliquots (1 mg) of EquC1 purified from different samples of horse sweat were extracted with ~1 mL of pentane, and the solvent was evaporated under nitrogen and the residue redissolved in 50 μL of heptane to be analyzed by gas chromatography and mass spectrometry (GC−MS), using an HP5890A/HP5971A instrument. Gas chromatographic separations were performed on a Restek Rtx-5MS column using the following conditions: isotherm at 70 °C for 30 min, first gradient of 30 °C/min up to 150 °C, 5 min isotherm, then a second gradient of 5 °C/min to 310 °C, and final isotherm of 11 min. The injector was kept at 280 °C. Mass spectra were acquired between *m*/*z* 42 and 550.

Fluorescence Measurements. Emission fluorescence spectra were recorded on a Jasco FP-750 instrument at 25 °C in a right angle configuration, with a 1 cm light path quartz cuvette and 5 nm slits for both excitation and emission. The protein was dissolved in 50 mM Tris-HCl buffer (pH 7.4), while ligands were added as 1 mM methanol solutions.

Intrinsic Fluorescence. The tryptophan intrinsic fluorescence was measured on a 2 μM solution of the protein, using an excitation wavelength of 295 nm and recording the emission spectrum between 300 and 360 nm. Quenching of intrinsic fluorescence was assessed under the same condition and in the presence of *N*-phenyl-1-naphthylamine (1-NPN) at concentrations between 1 and 20 μM.

Binding Assays. To measure the affinity of the fluorescent ligand 1-NPN for the different proteins, a 2 μM solution of the protein in 50 mM Tris-HCl (pH 7.4) was titrated with aliquots of 1 mM ligand in methanol to a final concentration of 1−20 μM. The affinity of other ligands was measured in competitive binding assays, using 1-NPN as the fluorescent reporter at a concentration of 1 μM and concentrations of 1−6 μM for each competitor.

Data Analysis. To determine the binding constants, the intensity values corresponding to the maximum of fluorescence emission were plotted against free ligand concentrations. Bound ligand was evaluated from the values of fluorescence intensity assuming that the protein was 100% active, with a protein:ligand stoichiometry of 1:1 at saturation. The curves were linearized using Scatchard plots. Dissociation constants of the competitors were calculated from the corresponding IC_{50} values, using the equation $K_D = IC_{50}/(1 + [1\text{-NPN}])/K_{1-NPN}$, [1-NPN] being the free concentration of 1-NPN and K_{1-NPN} being the dissociation constant of the protein−1-NPN complex. In the case of EquC1, this value was 0.5 μM.

RESULTS

The presence of soluble pheromone carrier proteins in secretions such as saliva, sweat, urine, and vaginal discharge of several mammals prompted us to investigate such aspects in the horse. Here we report on the isolation and characterization of a salivary protein belonging to the PSP family, as well as structural and binding studies on a lipocalin, a major component of sweat, already described as an allergen and named EquC1.

Salivary Proteins. Electrophoretic analysis under denaturing conditions of crude extracts from the three major horse salivary glands (parotid, submaxillary, and sublingual) revealed the presence of an abundant component migrating

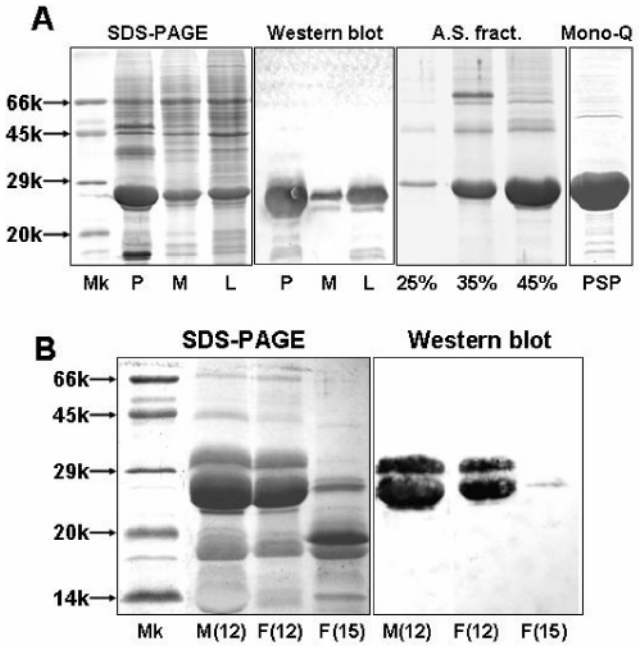

FIGURE 1: Western blot analysis and protein purification. (A) SDS−PAGE and Western blot analysis (antiserum against purified horse PSP) of crude extracts from parotid (P), submaxillary gland (M), and sublingual gland (L) of a male horse. The antiserum reacted with a major band present in all samples and migrating with an apparent mass of 28 kDa. Similar results were obtained with female samples. The 28 kDa protein was purified with ammonium sulfate (A.S.) fractionation, followed by anion exchange chromatography on a Mono-Q column. (B) Electrophoretic analysis of fractions eluted via gel filtration chromatography on Superose-12 of a crude sample of horse sweat and the corresponding Western blot analysis using pig-SAL antiserum. M(12) and F(12) represent fraction 12 from male (M) and female (F) individuals containing partially purified EquC1, respectively, as identified by MALDI-TOF mass fingerprint analysis. F(15) represents fraction 15 from female individuals containing latherin as a major component, as identified by MALDI-TOF mass fingerprint analysis (data not shown). Lane Mk contained molecular weight markers.

with an apparent mass of 28 kDa. This protein was most abundant in the parotid, and its presence was not dependent on sex. Figure 1A reports the electrophoretic separations relative to male glands; identical patterns were observed with female samples. The protein was purified from a male parotid gland by fractionation with ammonium sulfate, followed by anion exchange chromatography. A sample of the purified protein was used to immunize rabbits for polyclonal antibody production. These antibodies were used in Western blot experiments on crude extracts of the three glands, showing that the component at 28 kDa cross-reacted with the antiserum to the same extent in all three glands, in both male and female horses.

Purified samples of the 28 kDa protein from male and female individuals were reduced, alkylated, digested with trypsin, and submitted to peptide MALDI-TOF mass fingerprint analysis. They exhibited identical spectra, which unfortunately did not allow positive protein identification using different database searching algorithms (data not shown). Accordingly, peptide mixtures were resolved by microbore reversed phase HPLC, and homogeneous fractions, as verified by mass spectral analysis, were submitted to Edman degradation. Peptides with MH^+ at *m*/*z* 859.50, 1117.58, and 1446.73 were associated with the AVSSLVQR, GSLELQTDVR, and TIQDSEIWQQAK sequences, respectively. In parallel, a blotted sample of intact protein yielded the SFLEDLRGKLDNVFNKLKPDLE sequence. These data were used for homology search investigations, which demonstrated similarities with mammalian parotid secretory proteins.

These peptide fragments were used to design oligonucleotides for further PCR experiments. On the basis of the very good conservation of the signal peptides in PSPs of different species, we designed a degenerate primer encoding the first 11 amino acids of PSPs (ATGBTTCARCTTTGGAAACT-TGTTYTCYTGTG). At the 3′ end, we used a reverse primer containing an oligo-dT followed by a specific sequence utilized in the synthesis of cDNA (ATTCTAGAGCGGC-CGCGACATGT_{14}). We thus obtained an amplification product of ~1100 bp. Nested PCR experiments, using some of the primers designed on internal amino acid sequences, yielded electrophoretic bands of the expected lengths. The PCR product, ligated in pGEM and sequenced, yielded a single full-length sequence with an open reading frame of 750 bases (GenBank accession number DQ788676), encoding a protein of 249 amino acids (Figure 2, top panel). On the basis of protein sequencing data, we identified residues 1−19 as the signal peptide. This site of cleavage was also predicted by analysis of the sequence with Signal-P. Thus, the mature protein, which here we call horse PSP, contains 230 amino acids and shares with other members of the same family between 34 and 51% of its residues (Figure 2, top panel).

Sequence scanning for the occurrence of specific patterns, profiles, and motifs in horse parotid secretory protein did not yield significant results. The absence of post-translational modifications, i.e., glycosylation and phosphorylation, was confirmed by extensive peptide mass mapping experiments, which also verified 97.4% of the deduced protein sequence (Supporting Information). However, a direct mass measurement of the intact protein following alkylation with iodoacetamide under reducing/denaturing or denaturing conditions demonstrated the occurrence of cysteine residues involved in a disulfide bridge. In the first case, a molecular mass of 25 027.2 ± 1.9 Da was measured, which corresponded to the incorporation of three carboxamidomethyl groups (theoretical mass value of 25 025.6 Da); in the second case, the measured mass (24 910.7 ± 2.1 Da) was indicative of the introduction of a unique carboxamidomethyl moiety (theoretical mass value of 24 909.4 Da). Disulfide bridge assignment was carried out by enzymatic hydrolysis of the corresponding derivatives and MALDI-TOF-MS analysis of the resulting peptide mixtures. In the tryptic digest of the sample alkylated under denaturing and nonreducing conditions, MH^+ signals at *m*/*z* 2210.29 and 4104.10 were associated with carboxamidomethylated peptide 108−128 and peptides 139−170 and 196−202 linked by a disulfide bond between Cys155 and Cys198 (Figure 3A). This assignment was further confirmed by the disappearance of the signal assigned to S−S bridged peptides after incubation with dithiothreitol and appearance of the corresponding reduced species. As expected, this signal was absent in the digest of the sample alkylated under denaturing and reducing conditions (Figure 3B). Similar conclusions about the cysteine redox state were inferred from the MALDI-TOF spectrum of the sample alkylated under denaturing/nonre-

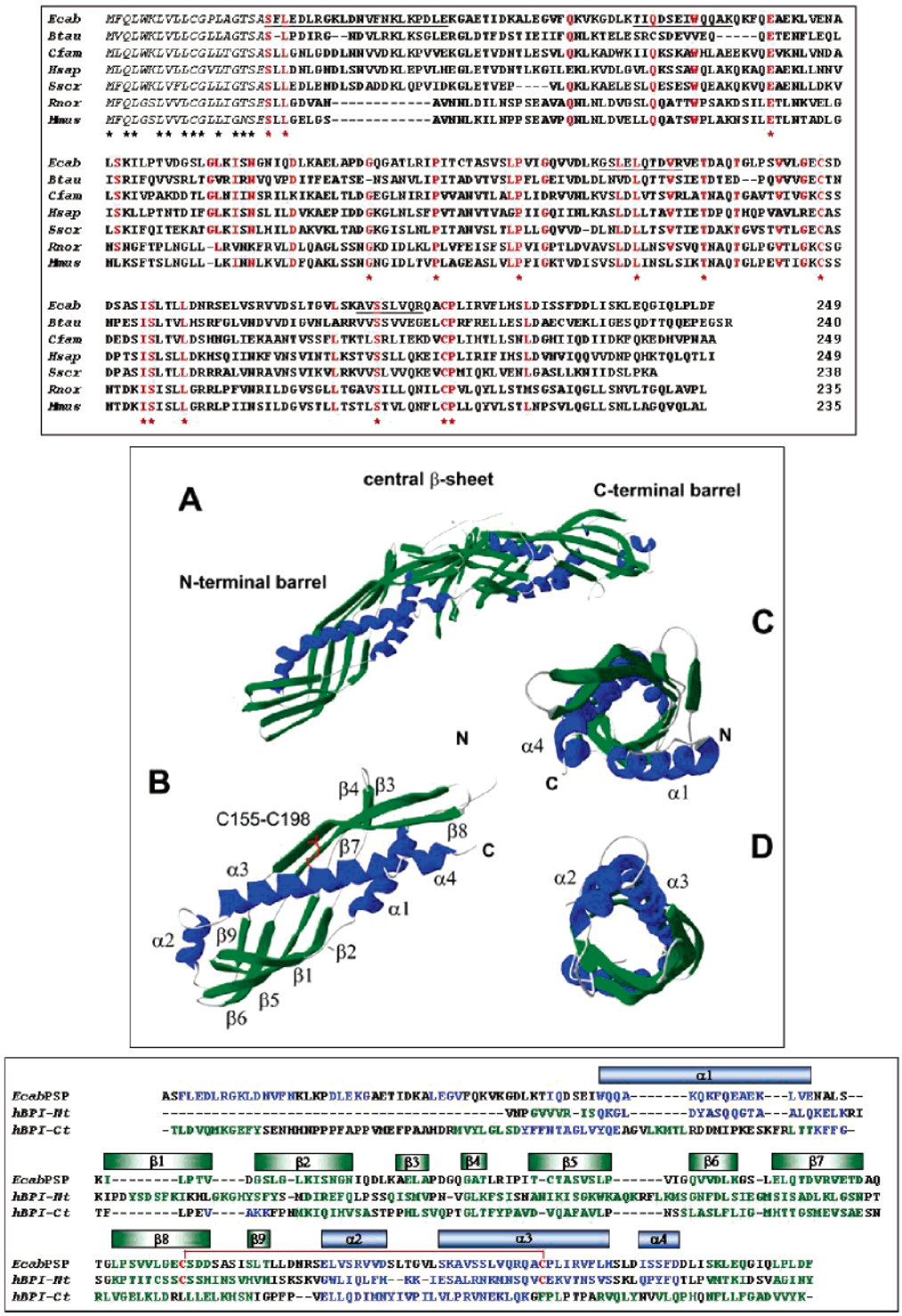

FIGURE 2: Amino acid sequence and three-dimensional model of horse PSP. In the top panel, the deduced full-length sequence is aligned with the other PSPs described in the literature: *Ecab*, horse; *Btau*, bovine; *Cfam*, dog; *Hsap*, human; *Sscr*, pig; *Rnor*, rat; and *Mmus*, mouse. Residues of horse PSP present in at least five other PSPs are colored red, and those that are fully conserved are also marked with an asterisk. Signal peptides are in italics. The horse PSP shares between 34 and 51% of its residues with the other PSPs. Sequences determined by Edman degradation are underlined. In the middle panel are three different views of the three-dimensional structure model of horse PSP. The model was constructed on the basis of the crystallographic structure of human BPI protein (PDB entry 1EWF) (A), using the secondary structure-driven sequence alignment reported in the bottom panel. On the basis of the highest degree of sequence homology, the N-terminal domain of BPI was used as a template. N-Terminal (residues 1−41) and C-terminal dodecapeptide fragments of horse PSP were not included in model construction. The horse PSP structure is reported from a lateral view of the barrel (B), a top view of the barrel facing the protein N- and C-termini (C), and a top view of the barrel burying the protein N- and C-termini (D). The β-sheet, helical, and loop regions are colored green, blue, and gray, respectively; they are annotated according to their progressive occurrence in polypeptide sequences. Amino acid residues involved in post-translational modification are annotated and highlighted in red. In the bottom panel is the secondary structure-driven sequence alignment of horse PSP with the N- and C-terminal domain of human BPI. The β-sheet and helical regions are colored green and blue, respectively.

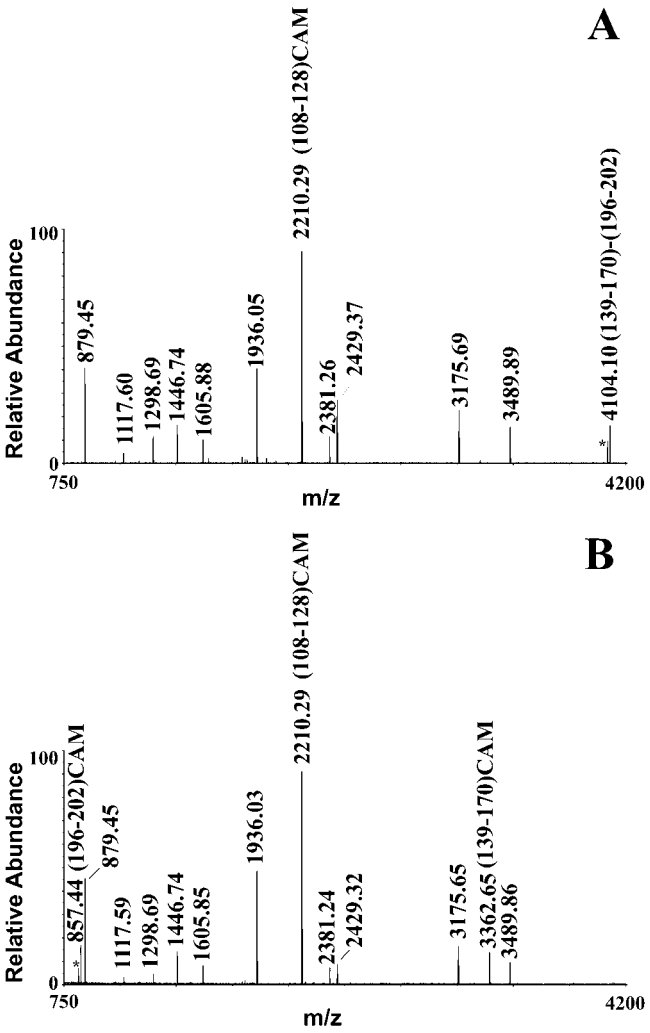

FIGURE 3: Cysteine redox state assignment of horse PSP. Tryptic digests of protein samples obtained following alkylation with iodoacetamide under denaturing and nonreducing (A) or denaturing and reducing (B) conditions were subjected to MALDI-TOF-MS analysis in reflectron mode. Peptides containing cysteine residues are selectively annotated. Asterisks indicate satellite peaks at *m*/*z* −17 Da resulting from partial cyclization of glutamine to 5-oxoproline during enzymatic hydrolysis.

ducing conditions following endoprotease AspN digestion, which showed MH^+ signals at *m*/*z* 2652.47 and 4711.84 associated with carboxamidomethylated peptide 100−125 and disulfide-containing peptide 142−156•179−208. In conclusion, these experiments unequivocally demonstrated that horse parotid protein contains Cys112 as a reduced amino acid residue and Cys155 and Cys198 joined by a S−S bridge.

Protein fold recognition analysis (*44*) identified human bactericidal permeability-increasing protein (BPI) (*45*) as the unique protein with a determined three-dimensional structure presenting a similar structural and domain organization. Horse PSP pairwise sequence alignment with N- and C-terminal domains of PBI gave only 11 and 12% levels of identity, respectively (Figure 2, bottom panel). Human BPI is a member of the PLUNC/LPS/LTP family, which has a highly elongated shape, consisting of two structurally similar domains nearly equal in size (Figure 2A). A barrel-like structural unit is found at each end of the protein, composed of a highly twisted, antiparallel β-sheet and two α-helices. The two barrels are bridged by a β-sheet in the center of the protein that contains residues from both the N- and C-terminal domains. In the N-terminal barrel, the two cysteine residues conserved in the LTP/LPS binding family form a disulfide bond that anchors the edge of the β-sheet to one of the α-helices. Each BPI domain has been demonstrated to behave as an independent folding module (*51*).

On the basis of the observed homology, conservation of the disulfide bridge, and secondary structure similarity, we hypothesized for horse PSP (Gly41−Ile217 sequence) a barrel fold similar to that occurring in the N-terminal domain of BPI. For the purpose of modeling, we generated a secondary structure-driven sequence alignment between the two proteins that was submitted to the modeling procedure (see Materials and Methods). Figure 2B shows the general folding pattern of the horse PSP molecule. The superimposed backbone trace with respect to the N-terminal domain of BPI displayed a 1.8 Å rmsd on 189 Cα atoms. The Ramachandran plots indicated that most of the residues (97%) exhibited φ and ψ angles in the core and allowed regions, except for Pro and Gly residues and a few amino acids located in loop regions (data not shown). Most bond lengths, bond angles, and torsion angles were in the range of values expected for a naturally folded protein (data not shown).

The schematic structural model consists of a typical nine-stranded β-barrel containing four helices (Figure 2B). The secondary structure elements identified in the PSP structure were α1 (Trp52−Glu67), β1 (Ile73−Val77), β2 (Gly79−Asn89), β3 (Glu96−Ala98), β4 (Gly103−Thr105), β5 (Thr111−Pro119), β6 (Gln123−Lys128), β7 (Glu132−Asp142), β8 (Leu147−Asp158), β9 (Ser163−Thr165), α2 (Glu172−Asp179), α3 (Ser186−His206), and α4 (Ile210−Asp214). This model revealed the presence of a long (55 Å) and narrow (10 Å) hydrophobic cavity inside the β-barrel able to accommodate linear molecules as the natural and synthetic ligands (Figure 2C,D). Accessibility to one side of the tunnel was partially controlled by Trp52, the first amino acid occurring on α1 (Figure 2C). A comparison of the models reported in the figure allowed us to highlight main structural differences among the horse protein and the N-terminal domain structure of human BPI. In fact, a careful analysis revealed the presence of shorter secondary structural elements (β1, β2, β5, and β6) in horse PSP, which affected the length of the barrel and accessibility to the cavity (Figure 2D).

Binding experiments performed with the fluorescent probe *N*-phenyl-1-naphthylamine showed a significant affinity of this ligand for the protein (K_D = 10 μM). The same compound also efficiently quenched the intrinsic tryptophan fluorescence of the protein (data not shown). However, competitive binding assays, performed with a large number of organic compounds, completely failed. Such putative ligands included small odorants, such as aliphatic alcohols of 6−10 carbon atoms, fatty acids of 12−18 carbon atoms and their amides, as well as a variety of aromatic molecules, both benzene derivatives and heteroaromatic compounds.

Sweat Proteins. Lipocalin EquC1 was already described as one of the major components of horse sweat and reported to be a powerful allergen. Its high degree of similarity, at the level of both amino acid sequence and three-dimensional structure, with MUPs and SALs, known to be carriers for specific pheromones, suggested the hypothesis that also EquC1 could perform a similar function. Accordingly, we

investigated the ligand binding characteristics of this protein. Although pheromones have not yet been identified in the horse, it is well-known that this species uses chemical cues to communicate with the other sex as well as for establishing hierarchy levels between males.

The similarity of EquC1 with pig SALs was confirmed also by a good cross-reactivity of the protein with anti-SAL antiserum (Figure 1B). This figure shows the electrophoretic separation of enriched proteins from male and female individuals. The antiserum against pig SAL strongly cross-reacted with two major bands in the samples, suggesting that two forms of EquC1 were present in sweat. Purified samples of both bands from male and female individuals were reduced, alkylated, digested with trypsin and PNGase F, and submitted to peptide MALDI-TOF mass fingerprint analysis. They exhibited identical spectra (data not shown), which allowed positive protein identification as EquC1. As a single sequence was reported for EquC1, the two observed protein bands were hypothesized to differ in the nature of present post-translational modifications. It was indeed reported that EquC1 is glycosylated and the bound oligosaccharides were characterized (*52*). Although two putative sites (Asn38 and Asn53) were predicted on the basis of specific motifs present within the EquC1 sequence, no direct assignment of the modification site(s) was achieved. Since glycosylation can strongly influence protein allergenic properties, we therefore decided to investigate the EquC1 glycosylation, in an attempt to provide definitive data.

A purified sample of EquC1 reduced and alkylated with iodoacetamide was subjected to trypsin digestion; the resulting digest was resolved by reversed phase HPLC, and all collected peptide fractions were submitted to MALDI-TOF-MS analysis. The occurrence of a specific fraction eluting at 28.7 min, which presented adjacent signals differing by *m*/*z* 162, 203, and 291 that disappeared after PNGaseF treatment, made glycopeptides immediately recognizable (Figure 4). In fact, signals in the *m*/*z* range of 1807.0−4831.7 were associated with glycosylated forms of peptide 50−63, as also confirmed by Edman degradation analysis. On the basis of the known biosynthetic pathway of N-linked oligosaccharides and the molecular mass of the peptide moiety, these signals were assigned to fragment 50−63 bearing complex type N-linked glycans bound to Asn53. A mixture of bi-, tri-, and tetra-antennary structures was confirmed, together with partially degraded oligosaccharide species probably generated by in-source MALDI fragmentation phenomena. Aliquots of nonglycosylated peptide 50−63 (MH^+ signal at *m*/*z* 1603.7) were also detected in the peak eluting at 37.1 min. These results, together with the ascertained occurrence of peptides 35−42 and 33−42 as nonglycosylated species (MH^+ signals at *m*/*z* 936.2 and 1193.4, respectively), demonstrated that a partial glycosylation occurred on Asn53 and no modification was present on Asn38.

On this basis, we concluded that the EquC1 bands observed in SDS−PAGE analysis were associated with a protein form not exhibiting post-translational modifications (having a lower molecular mass) and a protein form having bi-, tri-, and tetra-antennary oligosaccharide structures linked to Asn58 (having a higher molecular mass). Our results are in contrast with previously reported data showing only the occurrence of bi- and tri-antennary oligosaccharide structures with a reduced heterogeneity on EquC1 (*52*).

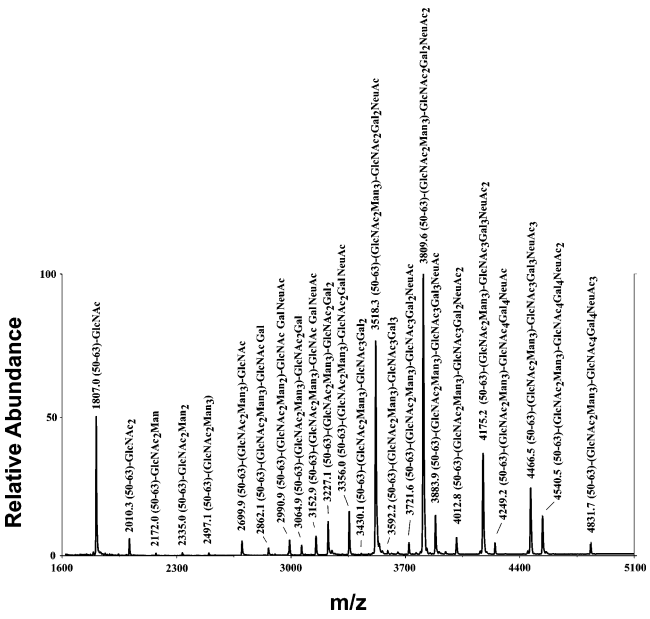

FIGURE 4: EquC1 glycan moiety structure and modification site elucidation. MALDI-TOF-MS analysis of the EquC1 tryptic digest fraction eluting at 28.7 min, which exhibited signals associated with glycopeptide isoforms. Assignment to glycosylated forms of peptide 50−63 was also demonstrated by direct Edman sequencing. The reported signals disappeared after PNGaseF treatment, which yielded a unique peptide with an MH^+ signal at *m*/*z* 1604.9, associated with the expected Asn53 → Asp conversion (data not shown). All spectra were recorded by using the instrument in a linear mode. Measured masses are reported as average values. $GlcNAc_2Man_3$, pentasaccharide core; Man, mannose; GlcNAc, *N*-acetylglucosamine; Gal, galactose; NeuAc, sialic acid.

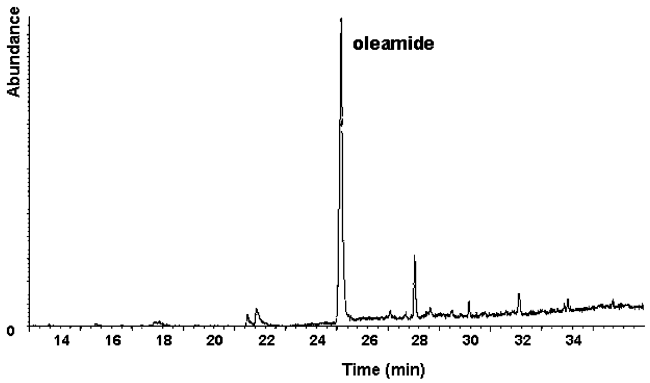

FIGURE 5: Gas chromatographic profile of a pentane extract from EquC1 purified from male horse sweat. The major peak in the chromatogram was identified as oleamide on the basis of its electron impact mass spectrum (data not shown).

On the basis of the similarity of EquC1 with pig SALs and mouse MUPs, we investigated the possible occurrence of endogenous ligands in this protein, which is similar to what was reported for the above-mentioned lipocalins. A pentane extract of the purified protein was subjected to gas chromatography−mass spectrometry (GC−MS) analysis. Figure 5 shows a typical profile obtained among those determined. The major observed peak was identified as oleamide following comparison of the fragmentation data with organic molecule databases. In other experiments, the extent and the number of minor peaks varied to a certain extent, but oleamide was always present as the most abundant component (data not shown).

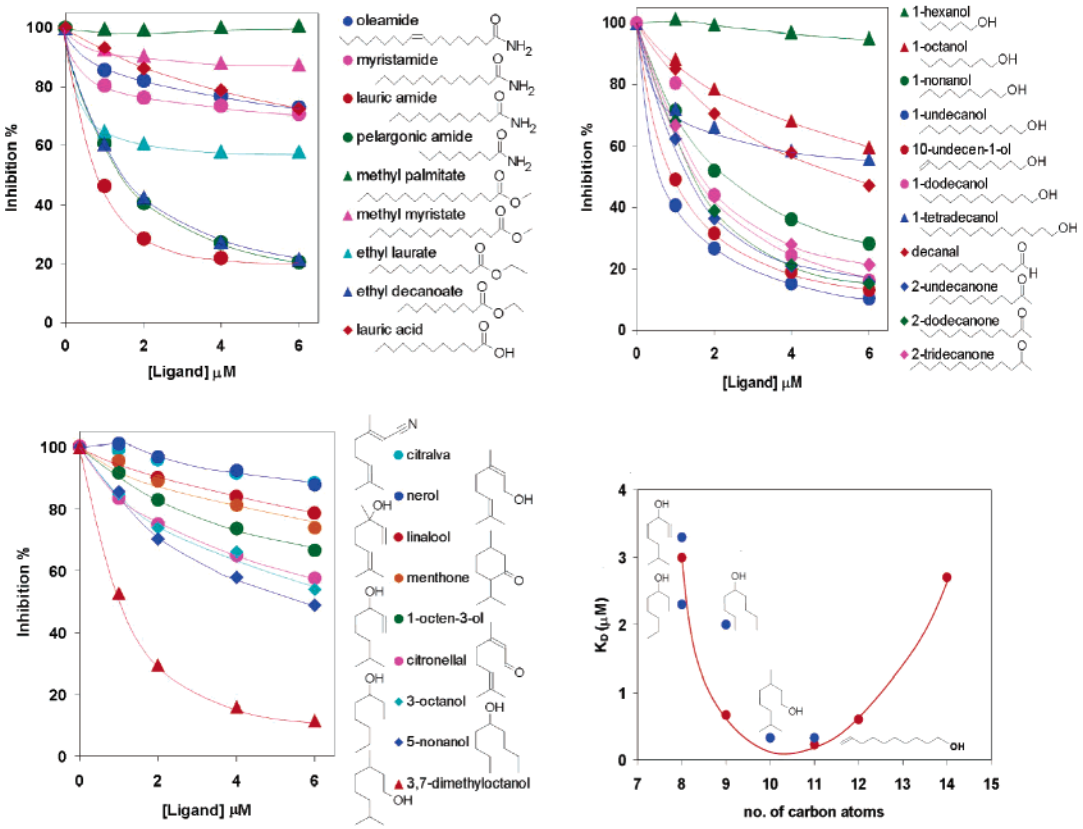

FIGURE 6: Binding of volatile compounds to a purified sample of EquC1. Aliquots (1 mL) of 2 μM protein in 50 mM Tris-HCl (pH 7.4) and 1 μM 1-NPN were titrated with 1−6 μM ligand, and the corresponding decrease in fluorescence was measured. The data are plotted as the percentage of the initial value of fluorescence before addition of the competing ligand. Dissociation constants of the competitors were calculated from the corresponding IC_{50} values, using the equation $K_D = IC_{50}/1 + [1\text{-NPN}]/K_{1-NPN}$, [1-NPN] being the free concentration of 1-NPN and K_{1-NPN} being the dissociation constant of the protein−1-NPN complex, which in our case was 0.5 μM. The bottom right panel reports K_D values for selected compounds to show the dependence of affinity on the length of the carbon chain and the position of the functional group. Red circles are data for linear saturated primary alcohols and blue circles for other alcohols, whose structures are reported.

Binding experiments, performed using a competitive fluorescent assay, revealed a certain affinity of the protein for oleamide. Different molecules were tested to identify structural determinants for protein effective binding. Representative results from binding experiments are reported in Figure 6, where ligands have been grouped by chemical classes. Binding of homologous linear amides from oleamide (C18) to pelargonic amide (C9) indicated that the best ligands were compounds having 9−12 carbon atoms (Figure 6A). A similar trend was apparent in the series of esters from methyl palmitate (C17) to ethyl decanoate (C12). The measured affinity of different linear alcohols (Figure 6B) also indicated the optimal size for efficient binding to be ~9−12 carbon atoms. Particularly interesting was the series of terpene derivatives (Figure 6C), including alcohols as well as aldehyde (citronellal) and nitrile (citralva) molecules. These results indicated that the binding was strongly affected by the flexibility of the molecule. In fact, the best ligand was 3,7-dimethyloctanol that, as an open fully saturated molecule, exhibits also the most flexible structure. Weaker binding data were measured with more rigid molecules, because of the presence of two double bonds (i.e., citralva, linalool, and nerol) or of a ring (i.e., menthone). Citronellal, containing a single unsaturation, exhibited medium affinity for the protein. The remaining alcohols, presenting the hydroxyl group in the middle of the chain, also exhibited reduced affinities. These results indicated that the presence of the functional group at the chain extremity is required for a good fitting. With aromatic molecules (i.e., eugenol, 2-phenylelthanol, and propiophenone), we were unable to measure any binding to EquC1 (data not shown).

In conclusion, the structural requirements for a good EquC1 ligand emerged: a medium-size molecule (9−12 carbon atoms) having a flexible structure and a functional moiety at position 1. The nature of the functional group (alcohol, amide, or ester) seemed to be rather irrelevant, but its position at one end of the chain appeared to be extremely important. Finally, methyl groups as side chains can be tolerated, as indicated by the strong affinity of 3,7-dimethyloctanol. The dependence of the affinity on the length of the chain can be visualized in Figure 6D, where the data relative to alcohols with different lengths and variable localization of the functional group are reported.

DISCUSSION

We have studied two proteins, representing the major components of horse saliva and sweat, as potential carriers of chemical messages within the species. The hypothesis was based on the knowledge that abundant salivary proteins carry both components of the pheromonal system in the boar (*11*), while human sweat contains strong odorants bound to proteins (*15*).

Parotid Secretory Protein. We found that the major salivary protein in the horse did not belong to the lipocalin

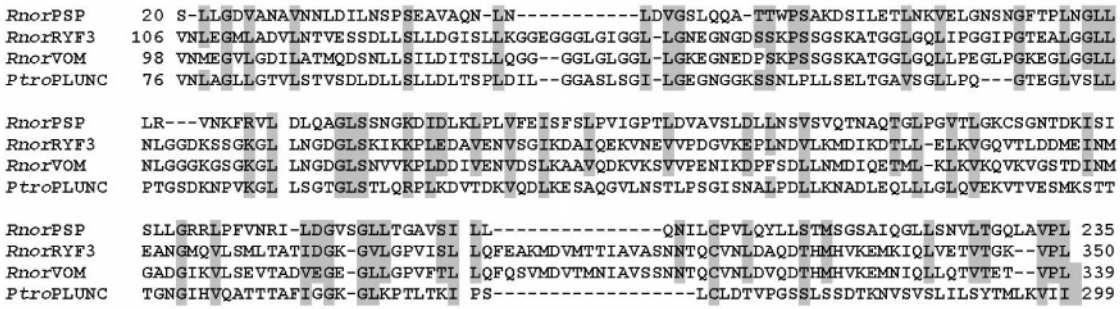

FIGURE 7: Alignment of rat PSP (*Rnor*PSP) with two proteins identified in the rat nasal area and proposed to ne involved in olfaction [RYF3 (*38*) and vomeromodulin (*39*)] and with a member (*Ptro*, *Pan troglodytes*) of the PLUNC family. This figure reports the complete mature rat PSP and only the regions involved in the alignment for the other proteins. The full-length sequences of rat RYP3, rat vomeromodulin, and chimpanzee PLUNC comprise 449, 436, and 350 amino acids, respectively. Residues of the rat PSP identical or similar in at least two of the three other proteins are highlighted. Similarity in this analysis is restricted to D and E; R and K; V, L, and I; and S and T.

group, as in the case of the pig, but to the PSP family, whose members have been isolated from the parotid of mouse (*29*), rat (*31*), pig (*34*), cow (*32*), and human (*33*). Their function is still not clear; sequence similarity with proteins of the BPI/PLUNC family has suggested that PSPs might be involved in the immune response (*32*). Various isoforms of PSP have been annotated in different genomes; as an example, the dog presents three PSP isoforms (GenBank accession numbers XM_845941, XM_857854, and XM_857878). It has also been observed that all PSPs reported in the literature contain a conserved N-myristoylation site and that pig and human PSPs also present an N-glycosylation site. In addition, pig, human, and bovine PSPs contain conserved phosphorylation sites for casein kinase II and protein kinase C. In this respect, it is interesting to observe that the horse PSP described in this study does not exhibit any post-translational modification, apart from a single disulfide bridge, or any potential modification site. Its function, therefore, could be unrelated to those proposed for the other proteins of the same family.

We have assessed saturating binding of 1-NPN to horse PSP, but then we did not observe any displacement of this fluorescent probe by a number of different linear ligands. It is likely that 1-NPN interacts with a superficial region of the protein and that the observed binding does not involve the protein hydrophobic cavity. This hypothesis is supported by titration experiments with 1-NPN, which efficiently quenched the tryptophan fluorescence. In fact, the unique Trp residue, present at position 52 and conserved in all except the bovine PSPs, appears to be located at the entrance and not inside the protein hydrophobic barrel (Figure 2). Proteins of the related BPI/PLUNC family have been reported to bind large elongated molecules such as phospholipids, which can be accommodated inside the long internal cavity in a stretched conformation. Our data cannot exclude the possibility that such compounds could also be the ligands for the horse PSP.

Finally, it is interesting to observe the peculiar similarity of PSPs to two proteins identified in the olfactory epithelium of the rat, namely, RYF3 (*38*) and vomeromodulin (*39*), both proposed to be odorant carriers. Although alignment required several amino acid insertions, these two polypeptides and rat PSP seem to exhibit sequence homology and conserved amino acid residues with members of the LPS/LTP/PLUNC family (Figure 7). On the basis of such similarity, the proposed role for RYF3/vomeromodulin, and the observed binding cavity in the PSP model, it is tempting to hypothesize a role of the semiochemical carrier also for horse PSP, although more ligand binding data as well as more information about the nature of semiochemicals in the horse are needed.

Sweat Lipocalin EquC1. Lipocalin EquC1, the major component of horse sweat, had been described as a potent allergen. In addition to studies on its allergenic properties (*25*, *26*), this protein had been subjected to an intensive structural characterization (*27*, *28*, *52*). The results reported in this paper definitively demonstrate the occurrence of a unique glycosylation site (Asn58) in the protein and the nature of the bound oligosaccharides. The EquC1 three-dimensional fold reproduces very closely the common β-barrel motif of lipocalins. The high degree of structural similarity with pig SALs, carriers of specific pheromones, also confirmed by a strong cross-reactivity with anti-SAL antibodies, prompted us to investigate the binding properties of this protein. To collect information about this aspect, we searched for endogenous ligands of EquC1 and, at the same time, we measured the binding affinity of the protein for a number of different potential ligands.

Several experiments aimed at the identification of organic molecules bound to the protein purified from horse sweat yielded variable results. In some cases, the only ligand detected was oleamide, while in other samples, we identified other compounds in different relative amounts. Anyway, oleamide was always present, often as the major component. Ligand binding experiments confirmed the affinity of the protein for oleamide but identified medium-length linear compounds as the ideal ligands for EquC1. The variability of the GC−MS profiles obtained with different protein extract samples may indicate that the composition of sweat with regard to volatile compounds, potential ligands for EquC1, probably depends on several factors, such as the physiological condition of the horse, the cause that produced sweating, and the site of collection on the animal body. This hypothesis found a counterpart in apolipoprotein-D, another protein carrier of potential semiochemicals identified in human sweat. When isolated from human sweat, apolipoprotein-D carries as an endogenous ligand a molecule with a very strong acrid odor, 2-methyl-3-heptenoic acid (*15*, *24*). Such an observation has suggested the hypothesis that this odor and its binding protein could be elements of a chemical communication system in humans, whose importance however was lost during evolution. A more detailed investigation, taking into account all these variables, in addition to sex and

age, could reveal particular chemicals that are secreted in horse sweat under certain conditions, representing chemical signals released by the animal in the environment.

On the other hand, our ligand binding experiments showed a clear trend that allowed the identification of structural requirements for a good fit to the protein. The most significant results of the binding experiments are summarized in Figure 6, where the plot of the measured dissociation constants versus the number of carbon atoms in the ligands is shown. The analysis of linear primary alcohols showed that the optimum length of the ligand clearly falls around 10−12 carbon atoms. A double bond at one end of the chain (as in the case of 10-undecen-1-ol), as well as the presence of two methyl groups as side chains (3,7-dimethyloctanol), is tolerated well, while the presence of internal double bonds or of the functional group in other positions of the chain greatly reduces the affinity for the protein. The first element probably acts by reducing the flexibility, and therefore the adaptability, of the ligand; the second one may drastically modify the oriented profile of the molecule. Provided the above requirements are assured, the nature of the functional group seems of minor relevance, as indicated by the good affinities of linear amides, esters, and ketones of 9−12 carbon atoms.

SUPPORTING INFORMATION AVAILABLE

MALDI-TOF-MS analysis of horse PSP alkylated under denaturing and reducing conditions and subjected to digestion with trypsin or endoprotease AspN. This material is available free of charge via the Internet at http://pubs.acs.org.

REFERENCES

1. Cavaggioni, A., and Mucignat-Caretta, C. (2000) Major urinary proteins, α_{2U}-globulins and aphrodisin, *Biochim. Biophys. Acta 1482*, 218−228.
2. Pelosi, P. (2001) The role of perireceptor events in vertebrate olfaction, *Cell. Mol. Life Sci. 58*, 503−509.
3. Cavaggioni, A., Findlay, J. B. C., and Tirindelli, R. (1990) Ligand binding characteristics of homologous rat and mouse urinary proteins and pyrazine binding protein of the calf, *Comp. Biochem. Physiol. 96B*, 513−520.
4. Bacchini, A., Gaetani, E., and Cavaggioni, A. (1992) Pheromone-binding proteins in the mouse *Mus musculus*, *Experientia 48*, 419−421.
5. Robertson, D. H. L., Beynon, R. J., and Evershed, R. P. (1993) Extraction, characterization and binding analysis of two pheromonally active ligands associated with major urinary protein of house mouse (*Mus musculus*), *J. Chem. Ecol. 19*, 1405−1416.
6. Böcskei, Z., Groom, C. R., Flower, D. R., Wright, C. E., Phillips, E. V., Cavaggioni, A., Findlay, J. B. C., and North, A. C. T. (1992) Pheromone binding to two rodent urinary proteins revealed by X-ray crystallography, *Nature 360*, 186−188.
7. Hurst, J. L., Payne, C. E., Nevison, C. M., Marie, A. D., Humphries, R. E., Robertson, D. H. L., Cavaggioni, A., and Beynon, R. J. (2001) Individual recognition in mice mediated by major urinary proteins, *Nature 414*, 631−634.
8. Singer, A. G., Macrides, F., Clancy, A. N., and Agosta, W. C. (1986) Purification and analysis of a proteinaceous aphrodisiac pheromone from hamster vaginal discharge, *J. Biol. Chem. 261*, 13323−13326.
9. Henzel, W. J., Rodriguez, H., Singer, A. G., Stults, J. T., Macrides, F., Agosta, W. C., and Niall, H. (1988) The primary structure of aphrodisin, *J. Biol. Chem. 263*, 16682−16687.
10. Briand, L., Huet, J.-C., Perez, V., Lenoir, G., Nespoulous, C., Boucher, Y., Trotier, D., and Pernollet, J.-C. (2000) Odorant and pheromone binding by aphrodisin, a hamster aphrodisiac protein, *FEBS Lett. 476*, 179−185.
11. Marchese, S., Pes, D., Scaloni, A., Carbone, V., and Pelosi, P. (1998) Lipocalins of boar salivary glands binding odours and pheromones, *Eur. J. Biochem. 252*, 563−568.
12. Loebel, D., Scaloni, A., Paolini, S., Fini, C., Ferrara, L., Breer, H., and Pelosi, P. (2000) Cloning, post-translational modifications, heterologous expression, ligand-binding and modelling of boar salivary lipocalin, *Biochem. J. 350*, 369−379.
13. Scaloni, A., Paolini, S., Brandazza, A., Fantacci, M., Marchese, S., Navarrini, A., Fini, C., Bottiglieri, C., Ferrara, L., and Pelosi, P. (2001) Purification, cloning and characterisation of novel odorant-binding proteins in the pig, *Cell. Mol. Life Sci. 58*, 823−834.
14. Spinelli, S., Vincent, F., Pelosi, P., Tegoni, M., and Cambillau, C. (2002) Boar salivary lipocalin. Three-dimensional X-ray structure and androsterol/androstenone docking simulations, *Eur. J. Biochem. 269*, 2449−2456.
15. Zeng, C., Spielman, A., Vowels, B. R., Leyden, J., Biemann, K., and Preti, G. (1996) A human axillary odorant is carried by apolipoprotein D, *Proc. Natl. Acad. Sci. U.S.A. 93*, 6626−6630.
16. Finlayson, J. S., Asofsky, R., Potter, M., and Runner, C. C. (1965) Major urinary protein complex of normal mice: Origin, *Science 149*, 981−982.
17. Shaw, P. H., Held, W. A., and Hastie, N. D. (1983) The gene family for major urinary proteins: Expression in several secretory tissues of the mouse, *Cell 32*, 755−761.
18. Shahan, K. M., Denaro, M., Gilmartin, M., Shi, Y., and Derman, E. (1987) Expression of six mouse major urinary protein genes in the mammary, parotid, sublingual, submaxillary and lachrymal glands and in the liver, *Mol. Cell. Biol. 7*, 1947−1954
19. Pelosi, P., Baldaccini, N. E., and Pisanelli, A. M. (1982) Identification of a specific olfactory receptor for 2-isobutyl-3-methoxypyrazine, *Biochem. J. 201*, 245−248.
20. Cavaggioni, A., Sorbi, R. T., Keen, J. N., Pappin, D. J. C., and Findlay, J. B. C. (1987) Homology between the pyrazine-binding protein from nasal mucosa and major urinary proteins, *FEBS Lett. 212*, 225−228.
21. Utsumi, M., Ohno, K., Kawasaki, Y., Tamura, M., Kubo, T., and Tohyama, M. (1999) Expression of major urinary protein genes in the nasal glands associated with general olfaction, *J. Neurobiol. 39*, 227−236.
22. Vincent, F., Lobel, D., Brown, K., Spinelli, S., Grote, P., Breer, H., Cambillau, C., and Tegoni, M. (2001) Crystal structure of aphrodisin, a sex pheromone from female hamster, *J. Mol. Biol. 305*, 459−469.
23. Briand, L., Blon, F., Trotier, D., and Pernollet, J. C. (2004) Natural ligands of hamster aphrodisin, *Chem. Senses 29*, 425−430.
24. Spielman, A., Zeng, X. N., Leyden, J., and Preti, G. (1995) Proteinaceous precursors of human axillary odor: Isolation of two novel odor-binding proteins, *Experientia 51*, 40−47.
25. Dandeu, J.-P., Rabillon, J., Carmi-Leroy, A., Divanovic, A., Camoin, L., and David, B. (1995) Equ c1, the horse major allergen and its close structural relationship to the mouse and rat major urinary protein, *J. Allergy Clin. Immunol. 95*, 348.
26. Gregoire, C., Rosinski-Chupin, I., Rabillon, J., Alzari, P. M., David, B., and Dandeu, J.-P. (1996) cDNA cloning and sequencing reveal the major horse allergen Equc1 to be a glycoprotein member of the lipocalin superfamily, *J. Biol. Chem. 271*, 32951−32959.
27. Bulone, V., Krogstad-Johnsen, T., and Smestad-Paulsen, B. (1998) Separation of horse dander allergen proteins by two-dimensional electrophoresis. Molecular characterisation and identification of Equ c 2.0101 and Equ c 2.0102 as lipocalin proteins, *Eur. J. Biochem. 253*, 202−211.
28. Lascombe, M., Gregoire, C., Poncet, P., Tavares, G., Rosinski-Chupin, I., Rabillon, J., et al. (2000) Crystal structure of the allergen Equc 1: A dimeric lipocalin with restricted IgE-reactive epitopes, *J. Biol. Chem. 275*, 21572−21577.
29. Madsen, H. O., and Hjorth, J. P. (1985) Molecular cloning of mouse PSP mRNA, *Nucleic Acids Res. 13*, 1−13.
30. Shaw, P., and Schibler, U. (1986) Structure and expression of the parotid secretory protein gene of mouse, *J. Mol. Biol. 192*, 567−576.
31. Gupta, N., Asp, E., Levan, G., and Mirels, L. (2000) Structure and chromosomal localization of the rat salivary Psp and Smgb genes, *Gene 243*, 11−18.
32. Wheeler, T. T., Hood, K., Oden, K., McCracken, J., and Morris, C. A. (2003) Bovine parotid secretory protein: Structure, expression and relatedness to other BPI (bactericidal/permeability-increasing protein)-like proteins, *Biochem. Soc. Trans. 31*, 781−784.

33. Geetha, C., Venkatesh, S. G., Dunn, B. H., and Gorr, S. U. (2003) Expression and anti-bacterial activity of human parotid secretory protein (PSP), *Biochem. Soc. Trans. 31*, 815−818.
34. Yin, H. F., Zhao, Z. H., Fan, B. L., Liu, Z. L., Lu, W., Liu, Y. F., and Li, N. (2004) cDNA cloning, genomic structure, chromosomal mapping, and expression analysis of parotid secretory protein in pig, *Genomics 83*, 9−18.
35. Wheeler, T. T., Haigh, B. J., McCracken, J. Y., Wilkins, R. J., Morris, C. A., and Grigor, M. R. (2002) The BSP30 salivary proteins from cattle, LUNX/PLUNC and von Ebner's minor salivary gland protein are members of the PSP/LBP superfamily of proteins, *Biochim. Biophys. Acta 1579*, 92−100.
36. Leclair, E. E. (2003) Four BPI (bactericidal/permeability-increasing protein)-like genes expressed in the mouse nasal, oral, airway and digestive epithelia, *Biochem. Soc. Trans. 31*, 801−805.
37. Robinson, C. P., Bounous, D. I., Alford, C. E., Nguyen, K. H., Nanni, J. M., Peck, A. B., and Humphreys-Beher, M. G. (1997) PSP expression in murine lacrimal glands and function as a bacteria binding protein in exocrine secretions, *Am. J. Physiol. 272*, G863−G871.
38. Dear, T. N., Campbell, K., and Rabbitts, T. H. (1991) Molecular cloning of putative odorant-binding and odorant-metabolizing proteins, *Biochemistry 30*, 10376−10382.
39. Khew-Goodall, Y., Grillo, M., Getchell, M. L., Danho, W., Getchell, T. V., and Margolis, F. L. (1991) Vomeromodulin, a putative pheromone transporter: Cloning, characterization, and cellular localization of a novel glycoprotein of lateral nasal gland, *FASEB J. 5*, 2976−2982.
40. Kyhse-Andersen, J. (1984) Electroblotting of multiple gels: A simple apparatus without buffer tank for rapid transfer of proteins from polyacrylamide to nitrocellulose, *J. Biochem. Biophys. Methods 10*, 203−209.
41. Vilardo, P. G., Scaloni, A., Amodeo, P., Barsotti, C., Cecconi, I., Cappiello, M., Lopez Mendez, B., Rullo, R., Dal Monte, M., Del Corso, A., and Mura, U. (2001) Thiol/disulfide interconversion in bovine lens aldose reductase induced by intermediates of glutathione turnover, *Biochemistry 40*, 11985−11994.
42. Allegrini, S., Scaloni, A., Ferrara, L., Pesi, R., Pinna, P., Sgarrella, F., Camici, M., Eriksson, S., and Tozzi, M. G. (2001) Bovine cytosolic 5′-nucleotidase acts through the formation of an aspartate 52-phosphoenzyme intermediate, *J. Biol. Chem. 276*, 33526−33532.
43. Gattiker, A., Gasteiger, E., and Bairoch, A. (2002) ScanProsite: A reference implementation of a PROSITE scanning tool, *Appl. Bioinf. 1*, 107−108.
44. Kelley, L. A., MacCallum, R. M., and Sternberg, M. J. E. (2000) Enhanced genome annotation using structural profiles in the program 3D-PSSM, *J. Mol. Biol. 299*, 501−522.
45. Kleiger, G., Beamer, L. J., Grothe, R., Mallick, P., and Eisenberg, D. (2000) The 1.7 Angstrom Crystal Structure of Bpi: A Study of How Two Dissimilar Amino Acid Sequences Can Adopt the Same Fold, *J. Mol. Biol. 299*, 1019−1034.
46. Huang, X., and Miller, W. (1991) A Time-Efficient, Linear-Space Local Similarity Algorithm, *Adv. Appl. Math. 12*, 337−357.
47. Pollastri, G., Przybylski, D., Rost, B., and Baldi, P. (2002) Improving the prediction of protein secondary structure in three and eight classes using recurrent neural networks and profiles, *Proteins 47*, 228−235.
48. McGuffin, L. J., Bryson, K., and Jones, D. T. (2000) The PSIPRED protein structure prediction server, *Bioinformatics 16*, 404−405.
49. Frishman, D., and Argos, P. (1995) Knowledge-based protein secondary structure assignment, *Proteins 23*, 566−579.
50. Hooft, R. W., Vriend, G., Sander, C., and Abola, E. E. (1996) Errors in protein structures, *Nature 381*, 272.
51. Beamer, L. J., Carroll, S. F., and Eisenberg, D. (1997) Crystal structure of human BPI and two bound phospholipids at 2.4 angstrom resolution, *Science 276*, 1861−1864.
52. Bulone, V., Rademaker, G. J., Pergantis, S., Krogstad-Johnsen, T., Smestad-Paulsen, B., and Thomas-Oates, J. (2000) Characterisation of horse dander allergen glycoproteins using amino acid and glycan structure analyses. A mass spectrometric method for glycan chain analysis of glycoproteins separated by two-dimensional electrophoresis, *Int. Arch. Allergy Immunol. 123*, 220−227.

BI061409P